INTERNATIONAL JOURNAL FOR NUMERICAL METHODS IN FLUIDS, VOL. 14, 167–173 (1992)

A NUMERICAL METHOD FOR THE DETERMINATION OF SLIP CHARACTERISTICS BETWEEN THE LAYERS OF A TWO-LAYER SLURRY FLOW

V. NASSEHI AND A. R. KHAN

Department of Chemical Engineering, Loughborough University of Technology, Loughborough, Leicestershire LE11 3TU, U.K.

SUMMARY

The observed phenomenon of slip between the layers of a flowing slurry is modelled mathematically by a finite-element-based numerical technique. This technique enables us to quantify variables such as the slip velocity and shear stress distribution at the interlayer boundary and the pressure drop within the flow domain.

KEY WORDS Finite element Interlayer slip Stress distribution Pressure drop

INTRODUCTION

Flow regimes involving the transport of solid particles by the motion of carrying liquids are referred to as slurry flows. A major difficulty in the analysis of such flows is the wide range of slurry conditions which may be encountered. These conditions vary from nearly homogeneous suspensions to regimes with a substantial proportion of solids forming a bed. Owing to this difficulty, it is not possible to find a generally applicable correlation for the pressure gradient in a slurry pipeline. Thus a universally reliable design method for such systems does not exist. On the one hand the behaviour of uniformly suspended solids in a liquid can be reasonably well described by that of a fluid of density equal to that of the mixture and viscosity equal to that of the liquid.[1] At the other end of the spectrum, where the solids predominantly settle down to the lower parts of the flow domain, there is a strong particle-to-wall friction which retards the flow at this section. In this case the most reasonable approach is to describe the flow regime as a two-layer one in which there is a liquid-on-liquid slip at the interlayer boundary. This view is enforced by the experimental observations which indicate that in these cases the location and shape of an interlayer boundary can be identified. Adopting this approach, many investigators have previously developed different two-layer slurry flow models.[2–4] These models are all based on a force balance between the upper and lower layers of the flow domain. The dominant force at the interlayer boundary is the liquid-to-liquid friction. In practice the relevant friction coefficient cannot be measured and a review of the developed two-layer models shows that they all rely on estimating the interfacial friction coefficient. Various methods for deriving such an estimate are suggested by the investigators.[3–5] However, owing to the lack of corroborative evidence, the reliability of all such estimates is in doubt. In this paper we present a numerical scheme which can be used at first instance to evaluate the accuracy of any given liquid-to-liquid friction model. This

0271–2091/92/020167–07$05.00 *Received February 1991*

scheme can be further employed to quantify unmeasurable variables such as the interlayer slip velocity and shear stress distribution in a two-layer flow regime. Our analysis is based on a two-dimensional slurry flow. The flow domain is divided into upper and lower parts. The upper layer flows faster than the lower layer and there is a slip boundary interface between the two parts. Variables such as geometrical dimensions, flow characteristics, exterior boundary conditions, material properties and the location and shape of the interfacial boundary used in this work are all based on previously published experimental data.[6] Early numerical experiments showed that for the case under study, owing to the relatively low viscosities, there is very little viscous heat generation and the temperature field within the flow domain remains constant. Thus here we present an isothermal analysis of the two-layer slurry flow.

MATHEMATICAL MODEL

In a Cartesian co-ordinate system the two-dimensional equations of continuity and motion representing the laminar, steady state, isothermal flow of non-Newtonian fluids are expressed as

$$\frac{\partial V_x}{\partial x}+\frac{\partial V_y}{\partial y}=0, \tag{1}$$

$$\rho V_x \frac{\partial V_x}{\partial x}+\rho V_y \frac{\partial V_x}{\partial y}=-\frac{\partial P}{\partial x}+\frac{\partial}{\partial x}\left(2\eta \frac{\partial V_x}{\partial x}\right)+\frac{\partial}{\partial y}\left[\eta\left(\frac{\partial V_x}{\partial y}+\frac{\partial V_y}{\partial x}\right)\right], \tag{2}$$

$$\rho V_x \frac{\partial V_y}{\partial x}+\rho V_y \frac{\partial V_y}{\partial y}=-\frac{\partial P}{\partial y}+\frac{\partial}{\partial x}\left[\eta\left(\frac{\partial V_x}{\partial y}+\frac{\partial V_y}{\partial x}\right)\right]+\frac{\partial}{\partial y}\left(2\eta \frac{\partial V_x}{\partial y}\right), \tag{3}$$

where V_x and V_y are the components of the velocity vector, P is the pressure and ρ is the material density. The shear-dependent viscosity η is defined in the present analysis by the following constitutive equation:

$$\eta=\eta_1[4\zeta_2(d)]^{(n-1)/2}, \tag{4}$$

where η_1 is a consistency (viscosity) coefficient, $\zeta_2(d)$ is the second invariant of the rate-of-deformation tensor[7] and n is a power-law index. Equations (1)–(4) together with the prescribed boundary conditions form the basis for the mathematical simulation described in this paper. It should be noted that in the present two-layer modelling of slurry flow the liquid motion in both the upper and lower layers is governed by the same equations, i.e. equations (1)–(4). Thus we need to derive only one set of working equations which, by adopting the appropriate boundary conditions, can be used to model the flow conditions in the upper or lower section of the domain.

WORKING EQUATIONS

A detailed derivation of the working equations of the present finite element scheme is given elsewhere[8] and will be only briefly described here. The two-dimensional flow domain is divided into an upper and a lower section. This division is such that there is a narrow width of overlap between the two layers. As is described in the next section, this narrow region is used to model the slip between the layers. The two parts of the flow domain are then discretized into meshes of finite elements using nine-noded biquadratic quadrilaterals (Figure 1). Variables within every element (Ω_e) are represented by the Lagrange interpolation model using relations such as

$$\tilde{V}_x=V_x^h=\sum_{i=1}^{m} N_i V_x^i, \text{ etc.}, \tag{5}$$

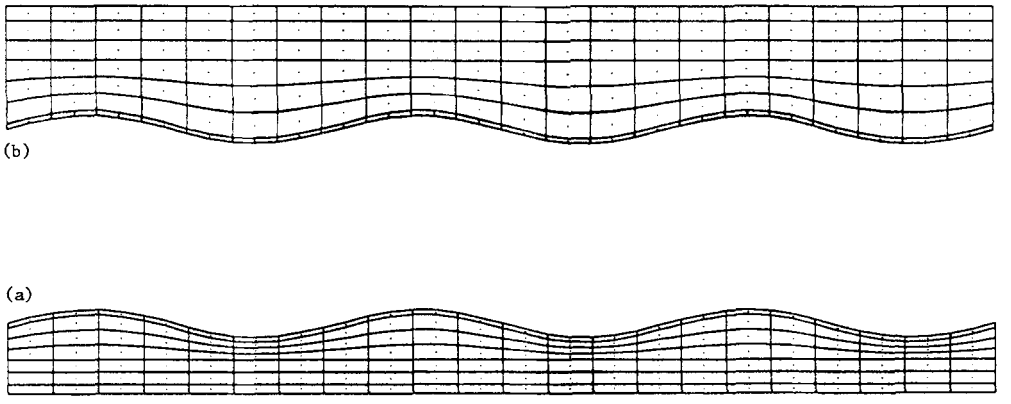

Figure 1. Finite element discretizations of (a) lower and (b) upper flow layers

where $\tilde{V}_x$ is a trial function representation of the variable V_x, V_x^h signifies the representation within the finite element, N_i is the interpolation function associated with node i, V_x^i is the nodal value of the variable V_x and m is the number of nodes per element. A weak variational form of the governing equations is then derived on the basis of the weighted residual Galerkin method incorporating a penalty function formulation. This process leads to the construction of the elemental stiffness equations which are used as the working equations in the present numerical scheme. Analogous to matrix forms with repetition on index i we have

$$
\begin{array}{|l|l|}
\hline
\displaystyle\int_{\Omega_e} \rho \bar{V}_x N_j \frac{\partial N_i}{\partial x}\,d\Omega_e & \displaystyle\int_{\Omega_e} \lambda \frac{\partial N_j}{\partial x}\frac{\partial N_j}{\partial y}\,d\Omega_e \\
+\displaystyle\int_{\Omega_e} \rho \bar{V}_y N_j \frac{\partial N_i}{\partial y}\,d\Omega_e & +\displaystyle\int_{\Omega_e} \eta \frac{\partial N_j}{\partial y}\frac{\partial N_i}{\partial x}\,d\Omega_e \\
+\displaystyle\int_{\Omega_e} (\lambda+2\eta)\frac{\partial N_j}{\partial x}\frac{\partial N_i}{\partial x}\,d\Omega_e & \\
+\displaystyle\int_{\Omega_e} \eta \frac{\partial N_j}{\partial y}\frac{\partial N_i}{\partial y}\,d\Omega_e & \\
\hline
\displaystyle\int_{\Omega_e} \lambda \frac{\partial N_j}{\partial y}\frac{\partial N_i}{\partial x}\,d\Omega_e & \displaystyle\int_{\Omega_e} \rho \bar{V}_x N_j \frac{\partial N_i}{\partial x}\,\partial\Omega_e \\
+\displaystyle\int_{\Omega_e} \eta \frac{\partial N_j}{\partial x}\frac{\partial N_i}{\partial y}\,d\Omega_e & +\displaystyle\int_{\Omega_e} \rho \bar{V}_y N_j \frac{\partial N_i}{\partial y}\,d\Omega_e \\
 & +\displaystyle\int_{\Omega_e} (\lambda+2\eta)\frac{\partial N_j}{\partial y}\frac{\partial N_i}{\partial y}\,d\Omega_e \\
 & +\displaystyle\int_{\Omega_e} \eta \frac{\partial N_j}{\partial x}\frac{\partial N_i}{\partial x}\,d\Omega_e \\
\hline
\end{array}
\begin{array}{l} v_x^i \\ \\ \\ \\ \\ v_y^i \\ \\ \\ \\ \end{array}
= \left\{ \begin{array}{l} \displaystyle\int_{\Gamma_e} N_j \eta \frac{\partial v_x^h}{\partial n}\,\partial\Gamma_e \\ \\ \\ \\ \\ \displaystyle\int_{\Gamma_e} N_j \eta \frac{\partial v_y^h}{\partial n}\,d\Gamma_e \end{array} \right\}, \qquad (6)
$$

$j=1, \ldots, m$, where Γ_e is the boundary confining Ω_e, $\vec{n}$ is the unit outward vector normal to Γ_e and $\bar{V}_x$, $\bar{V}_y$ are the old step values of the velocity components.

Using isoparametric mapping, this system of equations is cast in a suitable local co-ordinate system and the integrals on the left-hand sides are evaluated for every element. This evaluation is based on a selectively reduced Gaussian quadrature where the penalty terms (i.e. terms involving λ, the penalty parameter) are integrated using a lower number of integration points than the other terms.[9] The line integrals on the right-hand sides of the working equations vanish for all interelement boundaries and appear only on the exterior boundaries of the solution domain. Their appropriate treatment in any scheme is related to the nature of the boundary conditions to be used. A full discussion of boundary conditions used in our work is given later in the paper.

NUMERICAL SOLUTION SCHEME

The solution scheme starts by first considering one of the layers, say the lower layer. Using the working equations, the elemental stiffness equations for this section are derived and subsequently assembled. The resulting system of global equations becomes determinate after the imposition of the set of boundary conditions shown in Figure 2(a). To start the solutions at the upper boundary of the lower layer, an initial guess for the nodal velocities is given. The top thin layer of the elements at this section are 'virtual elements' used to model the slip condition. The concept of virtual elements has previously been applied for modelling convective heat flow boundary conditions[10] and later extended to model the momentum transfer in slip boundary situations.[8] In this method, to the outside of the actual domain a layer of thin elements known as 'virtual elements' is attached. The Dirichlet condition $V=V_b$ is then applied to the outer boundaries of these elements. The stress at the actual boundary is then related to the momentum transfer through the virtual elements, which are thin enough to allow the adoption of a linear momentum flux. Equating this virtual momentum flux to the required stress at the boundary, we get

$$lK_s(V_t-V_b)=\frac{\eta_v}{d_v}(V_t-V_b), \tag{7}$$

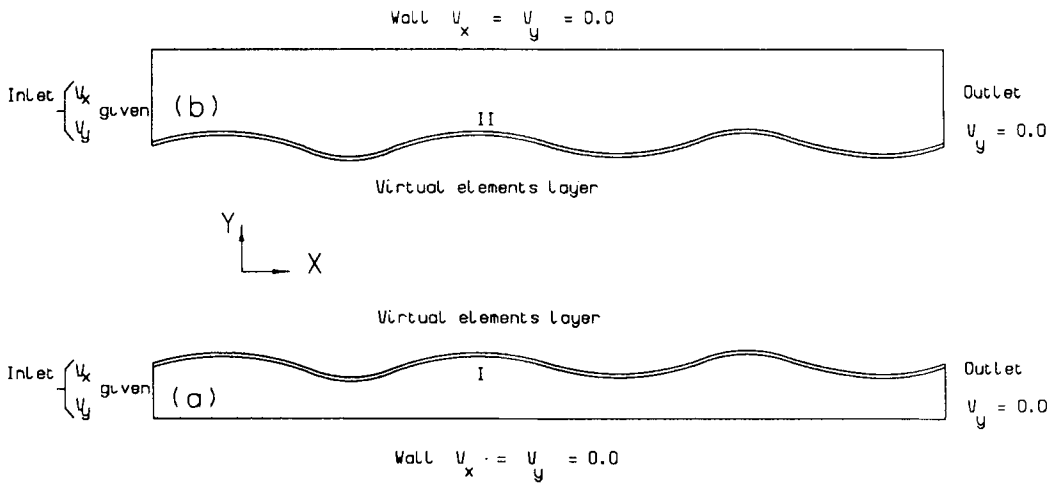

Figure 2. Boundary conditions and virtual element layers for (a) lower and (b) upper flow layers

where η_v and d_v are the appropriate virtual viscosity and thickness of the virtual elements respectively, l is the gap width of the flow domain, V_t is the tangential velocity along the domain boundary (i.e. the slip velocity to be calculated) and k_s is the coefficient of slip friction. Thus the virtual viscosity for a virtual element should be chosen as

$$\eta_v = K_s d_v l, \tag{8}$$

and for a curved surface the required result is

$$\eta_v = d_v \frac{R_w}{R_{lm}} K_s l, \tag{9}$$

where R_w is the local radius of curvature of the domain boundary and R_{lm} is the log-mean radius of the domain and virtual surfaces. In the present work we have taken d_v to be 0·001 m, which is thin enough to make our assumptions valid without generating any computational problems (i.e. elements with very high aspect ratios). K_s depends on the selected empirical liquid-on-liquid friction model. The selection of this coefficient is discussed in the next section. Imposing the described boundary conditions, the system of global equations for the lower section is solved. Since the flow regime is non-Newtonian, in order to obtain an accurate simulation of the flow field, the previous step is iterated, updating the viscosity via the constitutive equation. After the convergence of these iterations, the computed nodal velocities at the lower sides of the virtual elements are used as the boundary condition for the upper section, which in turn includes a layer of virtual elements at its lower boundary (Figure 2(b)). Imposition of the shown boundary conditions enables us to generate a velocity field for the upper section using an iterative procedure identical to that used for the lower part. Since these two layers overlap over the width of the virtual elements, it is possible to repeat the entire cycle until a converged flow field for the complete flow domain is obtained. In the present method all the used boundary conditions are of Dirichlet type and thus the solution scheme does not depend on the evaluation of the line integrals (equation (6)) on the slip boundaries. This makes the procedure simpler than the other methods used to simulate the slip wall conditions.[11] The converged velocity field is finally used to obtain the stress and pressure values within the flow domain via a variational recovery method.[7]

APPLICATION OF THE NUMERICAL TECHNIQUE

The described numerical algorithm can be employed to examine the validity of the liquid-on-liquid slip models suggested by different investigators. In order to do this, the friction coefficient K_s derived from the suggested models is used in the numerical scheme to obtain the pressure drop along the flow domain. The comparison between the computed and experimentally measured pressure drops provides a basis for the critical examination of the friction coefficient and subsequently the adopted liquid-to-liquid friction model. If this comparison proves to be satisfactory, the method can be used to produce unmeasurable values such as the interlayer velocity distribution and shear stress within the flow domain.

To illustrate the application of this method, we consider a slurry flow within a rectangular domain of 0·038 m width and 0·2 m length. The slurry consists of sodium carboxymethyl cellulose solution as the carrying liquid and gravel particles of 0·0057 m diameter as the suspended solid. We examine the case when the experimental observations show that there is a distinct interface between the upper and lower layers of the fluid at 0·0143 m above the base of the flow domain. In this case 21% wt of the lower part consists of solids.[76] The flow velocity is 0·23 m s^{-1} at the inlet of the domain. The material consistency η_1 is 0·83 and the power-law index n is 0·64. The fluid density at the upper layer is 1000 and at the lower layer is 1825 (SI units). According to the

observations, the interfacial boundary can be accurately represented by the following sinusoidal curve:

$$y = 0{\cdot}0143 + 0{\cdot}00285 \sin(30\pi x) \quad \text{for } 0 < x < 0{\cdot}2. \tag{10}$$

The experimentally measured pressure drop along this domain is 3095 Pa m^{-1}.[6] We start with a commonly used liquid-to-liquid friction model given as

$$K_s = 2/[3{\cdot}36 + 4\log_{10}(D/d)]^2, \tag{11}$$

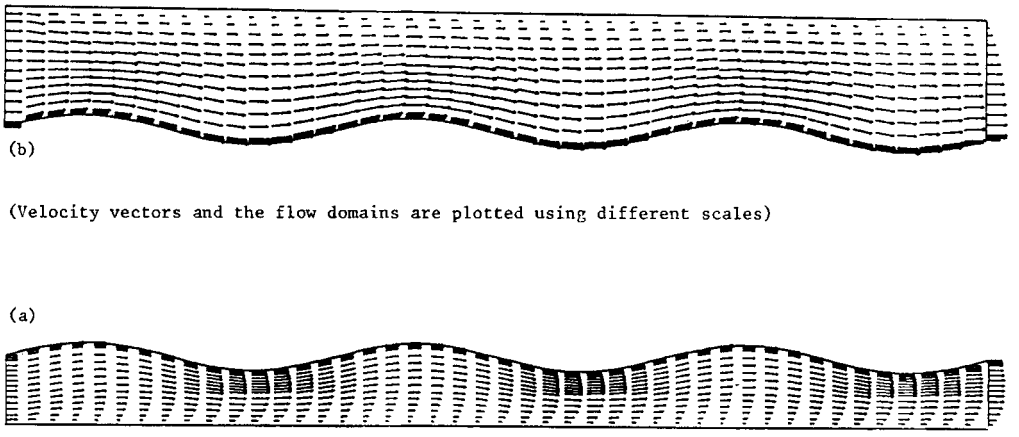

Figure 3. Simulated velocity fields for (a) lower and (b) upper flow layers

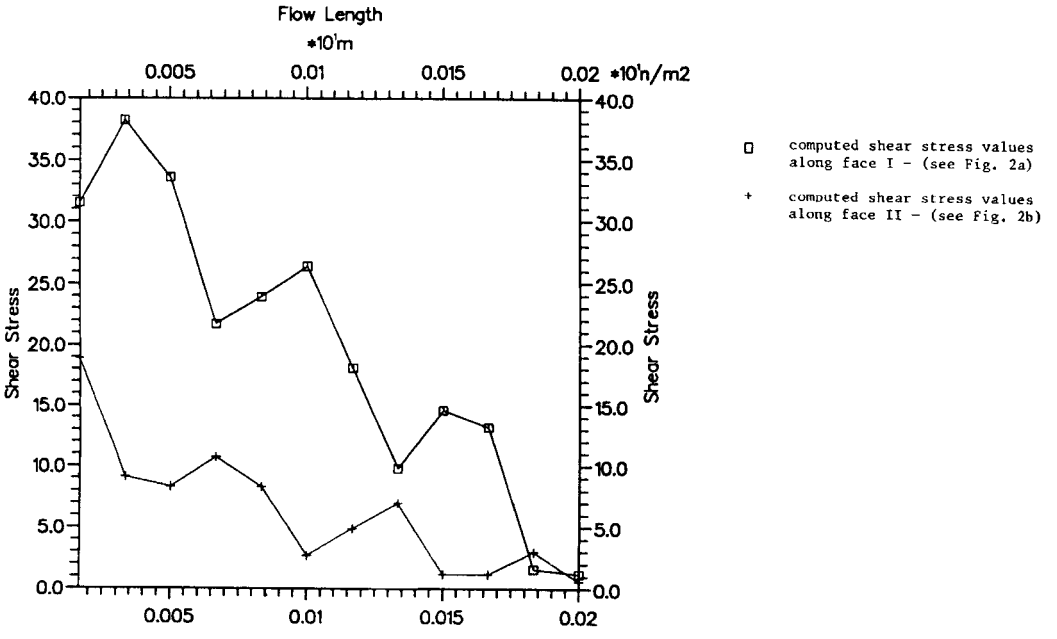

Figure 4. Shear stresses along lower and upper flow layers

where D/d is the ratio of domain to particle diameters.[3] Other investigators have suggested that the value of K_s from equation (11) should be modified by multiplying by $1+\gamma$, where

$$\gamma = \begin{cases} 0, & d/D < 0{\cdot}0015, \\ 4 + 1{\cdot}42 \log_{10}(d/D), & 0{\cdot}0015 < d/D < 0{\cdot}15. \end{cases} \tag{12}$$

However, these factors are tentative and are considered to be doubtful.[3] We start with a value of K_s calculated by equation (11) and use it to obtain a numerical pressure drop for the domain. This pressure drop is compared with the experimentally measured value. We then alter K_s until a satisfactory comparison is achieved. The final results show that only after multiplying K_s from equation (11) by a factor of 30 does the numerical model produce a pressure drop comparable to the measured value. This is nearly eight times the modification factor given by equation (12). On the basis of this value of K_s we obtain the velocity fields shown in Figure 3 and the shear stress along the interfacial boundary (Figure 4).

REFERENCES

1. G. W. Govier and K. Aziz, *The Flow of Complex Mixtures in Pipes*, Van Nostrand Reinhold, New York, 1972.
2. Y. Televantos, C. A. Shook, A. Carlton and M. Streat, 'Flow of slurries of coarse particles at high solid concentrations', *Can. J. Chem. Eng.*, **57**, 255–262 (1979).
3. C. A. Shook, L. Geller, R. G. Gillies, W. H. W. Husband and M. Small, 'Experiments with coarse particles in 250 mm pipeline', *10th Int. Conf. on Hydro Trans. of Solids in Pipes*, 1986, Paper f4, pp. 219–227.
4. P. Doron, D. Garnica and D. Barnea, 'Slurry flow in horizontal pipes—experimental and modelling', *Int. J. Multiphase Flow*, **13**, 535–547 (1987).
5. K. C. Wilson and N. P. Brown, 'Analysis of fluid friction in dense-phase pipeline flow', *Can. J. Chem. Eng.*, **60**, 83–86 (1982).
6. A. R. Khan, R. L. Pirie and J. F. Richardson, 'Heavy medium transport', *6th. Int. Conf. on Transport and Sedimentation of Solid Particles, Vol. 176*, 1988, pp. 187–198.
7. J. F. T. Pittman and S. Nakazawa, 'Finite element analysis of polymer processing operation', in J. F. T. Pittman, O. C. Zienkiewicz, R. O. Wood and J. M. Alexander (eds), *Numerical Analysis of Forming Processes*, Wiley, New York, 1984, Chap. 6, pp. 165–219.
8. V. Nassehi and P. K. Freakley, 'Spreader blade analogy of flow past an internal mixer rotor: two dimensional steady state model', *Int. Polym. Process.*, in the press.
9. T. J. R. Hughes, *The Finite Element Method*, Prentice-Hall, Englewood Cliffs, NJ, 1987.
10. J. F. T. Pittman, in C. L. Tucker (ed.), *Fundamentals of Computer Modelling for Polymer Processing*, Hanser, New York, 1990, Chap. 6.
11. W. J. Silliman and L. E. Scriven, 'Separating flow near a static contact line, slip at a wall and shape of a free surface', *J. Comput. Phys.*, **34**, 287–313 (1980).